

# Semi-insulating GaN by Fe-Doping in Hydride Vapor Phase Epitaxy Using a Solid Iron Source

Frank Lipski

*Using a solid iron source, Fe-doping during GaN growth by hydride vapor phase epitaxy (HVPE) on sapphire was realized. The doping concentration could be controlled by varying the gas flow over the iron source and was verified by secondary ion mass spectrometry (SIMS). After removal of the sapphire substrate, semi-insulating freestanding (FS) GaN of high quality was achieved, with a resistivity of up to  $4 \cdot 10^8 \Omega\text{cm}$  at room temperature. For Fe-doped samples on sapphire, a partial release of the high, compressive strain at room temperature has been observed. The measurement of the full-width-half-maximum (FWHM) of high resolution X-ray (HRXRD) rocking curves was hampered by the serious wafer bow for both GaN on sapphire and freestanding GaN. Nevertheless, we observed values for FS-GaN as low as 40 arcsec and 80 arcsec for the (002) and (102)-reflection, respectively.*

## 1. Introduction

In the past few years, tremendous progress in the fabrication of freestanding GaN substrates of 2" diameter has been achieved [1]. The mass production of GaN substrates is starting up. Laser diodes (LD) are nowadays commonly grown on freestanding GaN, showing far better performance compared to LDs on foreign substrates [2]. Commercially available GaN substrates are produced by hydride vapor phase epitaxy (HVPE) on foreign substrates like sapphire and separated thereof after growth. Currently, HVPE offers the best compromise of crystal quality, growth speed, investment, running costs and flexibility. Other favorite growth techniques for GaN substrates like high pressure growth [3], ammonothermal growth [4] and the Na-flux [5] method mainly suffer from far slower growth rates resulting in a time consuming development process and require high investment for upscaling to mass production.

However, nominally undoped high quality material obtained by HVPE generally shows a fairly high n-type conductivity due to background impurities, such as Si and O, which are unavoidable with the standard HVPE process [6]. While this is acceptable and even preferable for optoelectronic applications like LDs and LEDs with backside contacts, it is not suitable for GaN based electronics, where a degradation of the device performance due to parasitic capacitance or current leakage is noticeable. However, due to its potential use for high-power, high-frequency and high-temperature applications, there is a strong increase in the research on GaN based electronics, such as AlGaIn/GaN high electron mobility transistors. These activities are accompanied by an emerging demand for semi-insulating (SI) GaN wafers.

Although there is no way to completely prevent Si and O impurities in HVPE, semi-insulating GaN can still be achieved by additional doping of electron trapping centers. It has been shown that transition metals like Cr and Fe act as a deep acceptor in GaN and can be used to compensate the background donors [7,8].

For metal organic vapor phase epitaxy (MOVPE) ferrocene is used as Fe source typically. This metal organic precursor is not suited for use in HVPE, because ferrocene decomposes too early in hot wall reactors typically used in HVPE systems. For the investigations of this work, we have chosen solid iron as source which can be used similarly to the Ga source, creating the  $\text{FeCl}_2$  precursor inside the reactor chamber by an HCl-stream over elemental iron. We investigated the efficiency and controllability of such a kind of source as well as the crystal quality and electrical properties of the resulting Fe-doped GaN.

## 2. Experimental

The HVPE growth was performed in a commercial Aixtron single-wafer HVPE system with a horizontal quartz-tube, heated in a furnace with five zones. A 1:1 mixture of nitrogen and hydrogen was used as carrier gas, as it showed to minimize cracking [10]. Ammonia was applied as nitrogen precursor, while GaCl was used as precursor for the group-III element. It was formed inside the reactor by streaming HCl gas over a liquid Ga source heated to  $850^\circ\text{C}$  and injected directly above the substrate. In our system, two identical channels of this type are available and the second one was filled with a solid iron wire with a purity of 99.99% and a diameter of 1 mm. The HCl-flow in these two channels can be adjusted independently. With an additional dilution setup, the HCl-flow in the Fe channel could be diluted down to  $1 \cdot 10^{-3}$  sccm. In all experiments, the substrate temperature during growth was kept constant at  $1050^\circ\text{C}$  and the pressure of the reactor at 900 hPa.

The doping concentration was measured by secondary ion mass spectrometry (SIMS). Resistivity- and Hall-measurements were performed at room temperature with Van-der-Pauw geometry. The crystal quality and strain situation was analyzed by high resolution X-ray diffraction (HRXRD) and low temperature photoluminescence (PL) at 10 K.

For the HVPE growth, we used GaN templates on (0001) sapphire substrates with a slight misorientation towards the a-plane. These templates were grown with an Aixtron 200/4 RF-S system. First an oxygen doped AlN nucleation layer was deposited at a temperature of  $900^\circ\text{C}$  and afterwards covered with a GaN-layer of about  $2.5\ \mu\text{m}$ . For defect reduction and strain relaxation a very thin SiN-interlayer was deposited during the MOVPE process [9]. This interlayer was deposited after a GaN layer of 300 nm and overgrown with another  $2.2\ \mu\text{m}$  GaN. The SiN itself is less than one monolayer and leads to templates with strong compressive strain allowing crack-free growth of comparably thick HVPE layers on sapphire.

For the fabrication of freestanding GaN layers, the templates have been processed further prior to the HVPE growth. We were using a self-separation process, which takes place during cool-down from the growth temperature due to strong thermal forces, caused by the different thermal expansion coefficients of GaN and sapphire. To facilitate the separation, a predetermined breaking point is defined. We found that a dielectric mask of

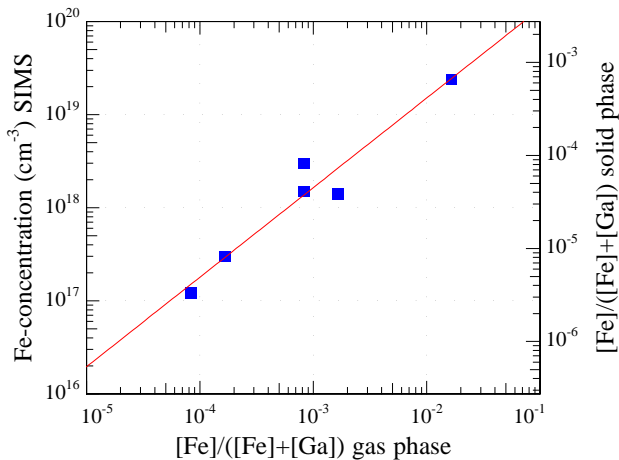


**Fig. 1:** Doping concentration measured by SIMS dependent on the concentration of Fe in the gas phase.

SiN dissolves during the HVPE process, leading to cavities in the GaN buffer below and finally to a defined separation. The SiN mask with a thickness of 200 nm was deposited by plasma enhanced vapor deposition (PECVD) on top of the templates described above. Afterwards, the mask was structured with a hexagonally shaped pattern by optical lithography and dry etching. Finally, a second MOVPE growth step was carried out before the templates were transferred to HVPE. Details of the separation process and its mask design can be found elsewhere [12].

### 3. Results and Discussion

The formation of  $\text{FeCl}_2$  by a HCl gas flow over solid iron is very efficient. In a first experiment we changed the amount of solid iron inside the reactor and measured the Fe-concentration in the grown samples by SIMS. Starting with some mm length, the measured Fe-concentration in the GaN samples increased with increasing wire length, but saturated when we reached several cm length. A further increase of the wire did not lead to a higher doping level. Consequently, we assume a total conversion of all HCl-molecules to  $\text{FeCl}_2$  for some cm length of the iron wire. For the GaCl-formation we assume a total conversion of all HCl-molecules of the 30 sccm-flow too, which allows to calculate the ratio of GaCl and  $\text{FeCl}_2$  in the gas phase. Based on this calculation, we found, that the incorporation of Fe-atoms into the crystal is not as efficient as it is for Ga-atoms. In Fig. 1 the compositions in gas phase and in solid phase are given. Nevertheless, in first experiments, the Fe concentration exceeded the values needed for compensation of background donors by several magnitudes. To realize the desired low Fe-concentrations, a dilution setup for the used HCl was required, enabling an improved control of the doping level. Moreover a reactor contamination by too much  $\text{FeCl}_2$  is avoided which could otherwise lead to background doping with Fe in later growth runs [13].

#### 3.1 Strain situation

When growing Fe-doped samples with HVPE, we noticed an increased cracking tendency for comparably thin layers of 30  $\mu\text{m}$ . A similar situation has been observed during our

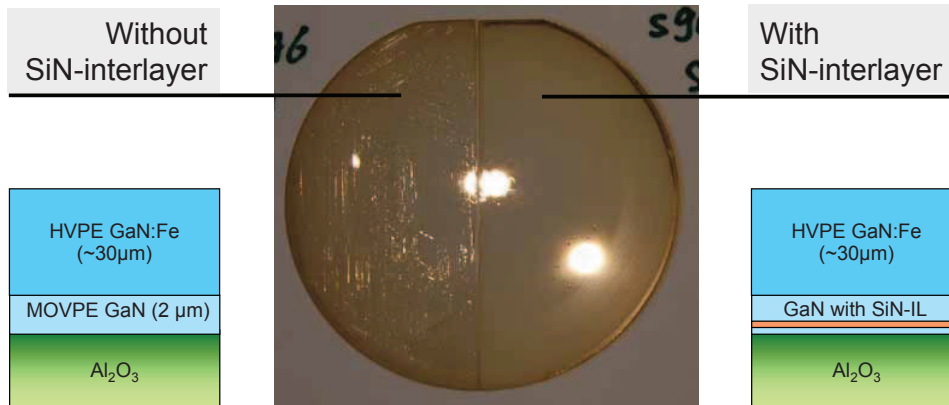


**Fig. 2:** 30  $\mu\text{m}$  thick Fe-doped GaN by HVPE. Two different templates of half a 2" wafer have been overgrown in the same HVPE run: the left one without SiN-interlayer, the right one with included SiN-layer.

studies on Si-doping by HVPE [14]. In that case, the introduction of a SiN monolayer during the template growth, typically applied for defect reduction, improved the situation dramatically and successfully helped to avoid cracking. The SiN interlayer leads to a higher compressive strain for GaN on sapphire at room temperature and consequently to a less tensile strain at growth temperature. Applying this technique in the case of Fe-doping the same effect was visible. A photograph of the results after an HVPE growth run of a 30  $\mu\text{m}$  thick GaN layer with a doping concentration of approx.  $1 \cdot 10^{19} \text{ cm}^{-3}$  is shown in Fig. 2. In this experiment, we used two different half wafers as a template, one with and one without the SiN interlayer described above. The sample with the SiN-interlayer shows a nice crack-free surface morphology, whereas the other shows many cracks already visible with bare eye.

A strain investigation by HRXRD for these samples is complicated due to the serious curvature, leading to big error bars for the lattice constants. Nevertheless, a tendency to a reduced compressive strain with increased Fe concentration is visible (Fig. 3). Further-

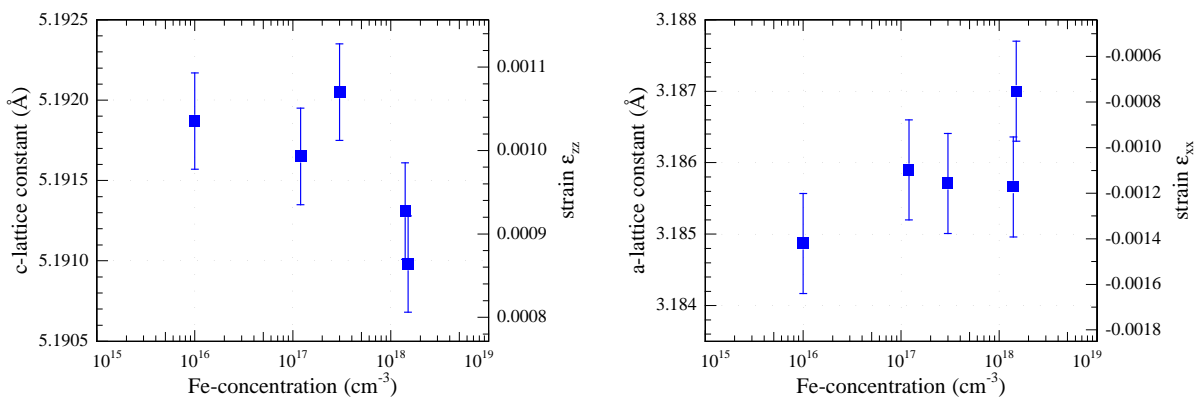


**Fig. 3:** Lattice constants determined by HRXRD-measuerments according to [16]. The strong bow leads to big error bars, nevertheless a reduced compressive strain for higher Fe-concentrations is noticeable.

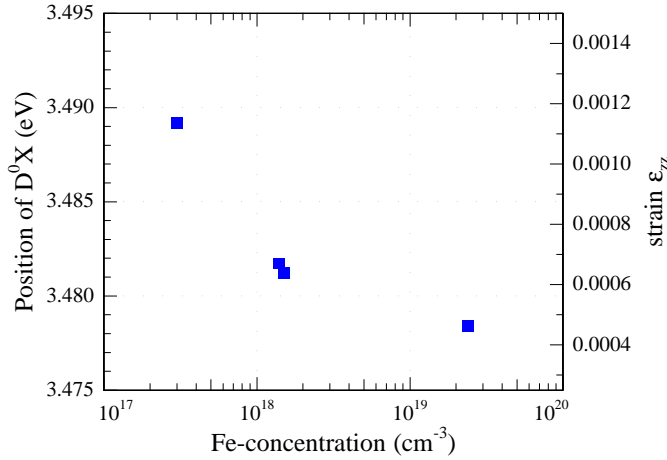


**Fig. 4:** PL measurements at 10 K of the donor-bound-exciton D<sup>0</sup>X provide accurate strain data.

more, we determined the strain more accurately by PL measurements of the position of the donor-bound-exciton D<sup>0</sup>X line (fig. 4). Unfortunately, the intensity of the D<sup>0</sup>X peak decreases with higher Fe-concentration and can even vanish totally, making the analysis difficult in this case. The strain values in the diagram have been calculated by solving the Hamilton operator according to [15]. The same tendency is clearly observable.

### 3.2 Crystal quality

At low doping concentrations, the surface morphology did not significantly change compared to undoped samples. Further increase of the Fe concentration lead to a degradation of the surface morphology starting from about  $1 \cdot 10^{19} \text{ cm}^{-3}$  (Fig. 5). Buried and overgrown cracks are visible at a doping concentration of  $1 \cdot 10^{20} \text{ cm}^{-3}$ .

An analysis of the crystal quality by HRXRD rocking curve measurements is hampered by the strong bow of the samples. The curvature of samples can lead to a broadening of measured FWHM similar to crystal imperfections like dislocations [17,18]. To distinguish between the different contributions to the broadening, a reduced beam size is required. Unfortunately, the X-ray system used for the measurements did not allow this reduction sufficiently.

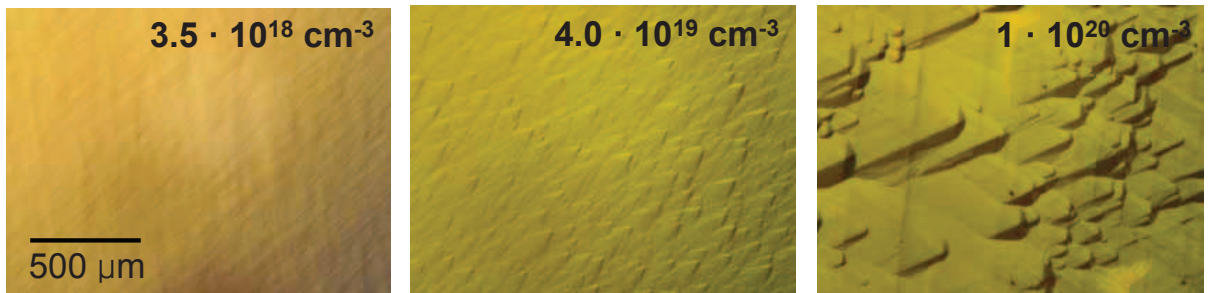


**Fig. 5:** Surfaces of differently doped samples from optical microscope in Nomarski contrast. For very high Fe concentrations, a degradation of the surface morphology is visible. On the sample with a Fe-concentration of more than  $1 \cdot 10^{20} \text{ cm}^{-3}$ , even some overgrown cracks are visible.

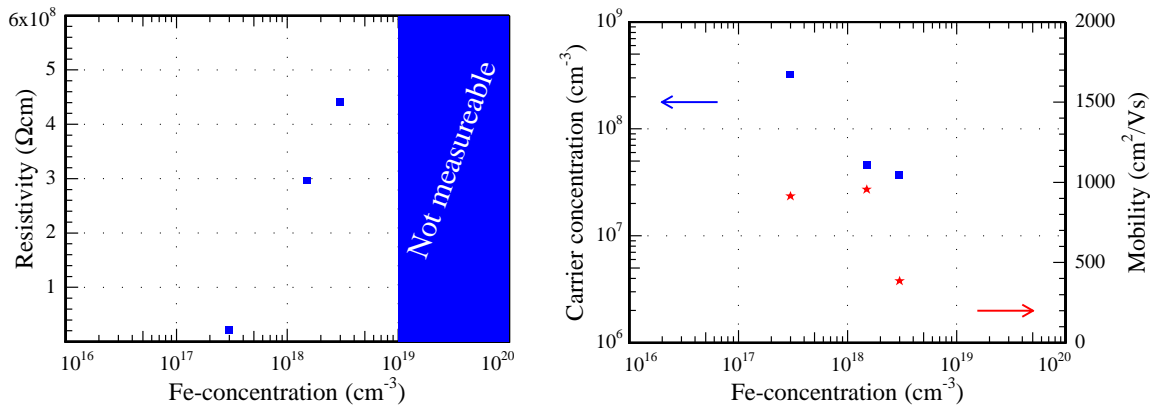


**Fig. 6:** Resistivity, carrier concentration and mobility of freestanding GaN dependent on the Fe-concentration, determined by RT-Hall measurements.

### 3.3 Electrical characterization

Resistivity measurements of the GaN samples on sapphire showed very low values due to a conductive layer at the interface to the sapphire by the O-doped AlN-nucleation as well as due to the included SiN-interlayer, acting as a kind of delta-doping. For accurate determination of the electrical properties of the HVPE GaN, the conductive layers must be removed. Therefore we have grown thick freestanding samples with a thickness of about 600  $\mu\text{m}$ . A controlled self-separation during cool-down can be achieved by including an additional SiN-interlayer [12]. In order to remove leftovers from the separation layer, the backsides of the freestanding samples have been mechanically polished. We could achieve resistivity values above  $4 \cdot 10^8 \Omega\text{cm}$  with a Fe concentration of about  $3 \cdot 10^{18} \text{cm}^{-3}$  after the removal of about 100  $\mu\text{m}$  [19]. Samples with even higher Fe concentration could not be measured with the used setup. In Fig. 6, resistivity values as well as resulting carrier concentrations and mobility values dependent on the doping concentration are shown.

## 4. Conclusion

Solid iron as source for Fe-doping in HVPE has been investigated. It is a simple and well controllable method for realizing SI-GaN by HVPE. To achieve the required doping concentrations, a dilution setup for the HCl stream is necessary. A degradation of the crystal quality due to the Fe doping was not observed for Fe-concentrations in the range of  $10^{18} \text{cm}^{-3}$ , which is approximately necessary for the compensation of background donors. Freestanding highly resistive GaN substrates with values up to  $4 \cdot 10^8 \Omega\text{cm}$  and above could be fabricated.

## Acknowledgement

I like to thank E. Richter of the Ferdinand-Braun-Institut für Höchstfrequenztechnik in Berlin for Hall-measurements and L. Kirste of the Fraunhofer-Institut für Angewandte Festkörperphysik in Freiburg for SIMS-measurements. Furthermore I want to thank H. Wu and W. Pang for their master theses on this topic.

## References

- [1] T. Paskova, D.A. Hanser, and K.R. Evans, “GaN substrates for III-nitride devices”, *Proc. IEEE*, vol. 98, pp. 1324–1338, 2010.
- [2] M. Furitsch, A. Avramescu, C. Eichler, K. Engl, A. Leber, A. Miler, C. Rumbolz, G. Brüderl, U. Strauß, A. Lell, and V. Härle, “Comparison of degradation mechanisms of blue-violet laser diodes grown on SiC and GaN substrates”, *phys. stat. sol. (a)*, vol. 203, pp. 1797–1801, 2006.
- [3] I. Grzegory, B. Lucznik, M. Bockowski, and S. Porowski, “Crystallization of low dislocation density GaN by high-pressure solution and HVPE methods”, *J. Cryst. Growth*, vol. 300, pp. 17–25, 2007.
- [4] R. Dwilinski, R. Doradzinski, J. Garczynski, L. Sierzputowski, R. Kucharski, M. Zajac, M. Rudzinski, R. Kudrawiec, J. Serafinczuk, and W. Strupinski, “Recent achievements in AMMONO-bulk method”, *J. Cryst. Growth*, vol. 312, pp. 2499–2502, 2010.
- [5] H. Yamane, M. Shimada, S.J. Clarke, and F.J. DiSalvo, “Preparation of GaN single crystals using a Na flux”, *Chemistry of Materials*, vol. 9, pp. 413–416, 1997.
- [6] Ch. Hennig, S. Hagedorn, T. Wernicke, G. Tränkle, M. Weyers, and E. Richter, “GaN substrates by HVPE”, *Proc. SPIE*, vol. 6910, pp. 69100I-1–10, 2008.
- [7] B. Monemar and O. Lagerstedt, “Properties of VPE-grown GaN doped with Al and some iron-group metals”, *J. Appl. Phys.*, vol. 50, pp. 6480–6491, 1979.
- [8] S. Heikman, S. Keller, S.P. DenBaars, and U.K. Mishra, “Growth of Fe doped semi-insulating GaN by metalorganic chemical vapor deposition”, *Appl. Phys. Lett.*, vol. 81, pp. 439–441, 2002.
- [9] J. Hertkorn, F. Lipski, P. Brückner, T. Wunderer, S.B. Thapa, F. Scholz, A. Chuvilin, U. Kaiser, M. Beer, and J. Zweck, “Process optimization for the effective reduction of threading dislocations in MOVPE grown GaN using in situ deposited SiN<sub>x</sub> masks”, *J. Cryst. Growth*, vol. 310, pp. 4867–4870, 2008.
- [10] E. Richter, Ch. Hennig, M. Weyers, F. Habel, J.D. Tsay, W.Y. Liu, P. Brückner, F. Scholz, Yu. Makarov, A. Segal, and J. Kaeppler, “Reactor and growth process optimization for growth of thick GaN layers on sapphire substrates by HVPE”, *J. Cryst. Growth*, vol. 277, pp. 6–12, 2005.

- [11] F. Scholz, P. Brückner, F. Habel, M. Peter, and K. Köhler, “Improved GaN layer morphology by hydride vapor phase epitaxy on misoriented Al<sub>2</sub>O<sub>3</sub> wafers”, *Appl. Phys. Lett.*, vol. 87, pp. 181902-1–3, 2005.
- [12] F. Lipski, T. Wunderer, S. Schwaiger, and F. Scholz, “Fabrication of freestanding 2”-GaN wafers by hydride vapour phase epitaxy and self-separation during cooldown”, *phys. stat. sol. (a)*, vol. 207, pp. 1287–1291, 2010.
- [13] W. Pang, “Investigations on Fe doping of GaN in hydride vapor phase epitaxy”, *Master Thesis, Ulm University*, 2009.
- [14] F. Lipski, “Si-doped GaN by hydride-vapour-phase-epitaxy using a Ga:Si-solution as doping source”, *Annual Report, Institute of Optoelectronics, Ulm University*, pp. 53–58, 2007.
- [15] D. Fu, R. Zhang, B. Wang, Z. Zhang, B. Liu, Z. Xie, X. Xiu, H- Lu, Y. Zheng, and G. Edwards, “Modification of the valence band structures of polar and nonpolar plane wurtzite-GaN by anisotropic strain”, *J. Appl. Phys.*, vol. 106, pp. 023714-1–8, 2009.
- [16] M.A. Moram, and M.E. Vickers “X-ray diffraction of III-nitrides”, *Reports on Progress in Physics*, vol. 72, pp. 036502-1–40, 2009.
- [17] M.A. Moram and M.E. Vickers and M.J. Kappers and C.J. Humphreys, “The effect of wafer curvature on x-ray rocking curves from gallium nitride films”, *J. Appl. Phys.*, vol. 103, pp. 093528-1–6, 2008.
- [18] J.E. Ayers, “The measurement of threading dislocation densities in semiconductor crystals by X-ray diffraction”, *J. Cryst. Growth*, vol. 135, pp. 71–77, 1994.
- [19] H. Wu, “Fabrication of Intentionally Doped Freestanding GaN layers by Hydride Vapor Phase Epitaxy”, *Master Thesis, Ulm University*, 2010.